Calibrating ASTER for Snow Cover Analysis

James Hulka

Department of Earth and Planetary Sciences, University of New Mexico, Albuquerque, New Mexico, USA
Center for Rapid Environmental Assessment and Terrain Evaluation (CREATE), University of New Mexico, Albuquerque, New Mexico, USA
Institute of Atmospheric Sciences, South Dakota School of Mines and Technology, Rapid City, South Dakota, USA

INTRODUCTION

A significant number of satellite instruments placed in orbit over the last few decades are able to acquire data for snow measurements. Global snow cover products have been available at coarse resolutions since the mid-1980s' launch of the Advanced Very High Resolution Radiometer (AVHRR) and Geostationary Operational Environmental Satellite (GOES) instruments. Global weekly data snow maps from these 1.1 km spatial resolution NOAA instruments have their origins back to the mid-1960s (Hall and Martinec, 1985).

The Earth Observing System (EOS) Terra spacecraft was launched in December 1999, and was followed two years later by Aqua. Scientists at the National Aeronautics and Space Administration (NASA) have been using data and images from the MODIS and ASTER instruments on board these satellites for atmospheric and environmental research projects. While many aspects of research have focused on land use, atmospheric aerosols, cloud cover, natural disasters, and biological emissions, a subset of projects has focused on cold weather processes. For many years, snow cover and snowfall, as well as ice thickness in the polar ice caps and small freshwater bodies, have been a point of interest but not always a primary research focus.

Snow cover data is very useful for delineating continental snow-covered areas, particularly in the Northern Hemisphere (Robinson et al., 1993). A wide array of MODIS products is available to users, many free of charge. In contrast to the continuous global coverage that MODIS provides, the ASTER also flies aboard the EOS Terra Spacecraft. This instrument provides high resolution, intermittent coverage over the same land and water surfaces, allowing for detailed analysis of the same regions covered by MODIS.

While remote sensing of snow has definitely experienced an improvement in spatial resolution since inception almost 40 years ago, there are a number of problems still present. The first NASA satellites had resolutions on the order of several kilometers. Today, operational satellites used for regional or global snow measurements exhibit spatial resolutions of as high as 500 meters, but lack sufficient information for determination of snow depth as well as edge detection of a snow pack. Data to determine these physical variables must be gathered from other sources in order to make a complete analysis. The visible-range sensors also are limited when clouds obstruct the view of the land surface while collecting data from orbit.

The purpose of this paper is to discuss the pre-processing of high-resolution ASTER data into reflectance by manually adjusting gain settings so that the results for the reflectance of pixels in each scene are representative of a snow spectrum. While moderate resolution data is sufficient for radiative transfer modeling on a global scale and for assessing continental-scale snow cover, it is insufficient for analyzing other hydrological processes. The ability to explore the processes that can only be observed with high-resolution data, such as the spring thaw and melt affecting water availability is a valuable tool that can assist modelers, scientists, and engineers in getting a better understanding of water cycles in river basins. A more detailed review of this work can be found in Hulka (2007).

METHODS

Fresh, pure snow has a very high spectral reflectance in the visible range (Wiscombe and Warren, 1981; O'Brien and Munis, 1975). However, age, impurities, thickness, and solar elevation can cause a significant decrease in these reflectance values (Wiscombe and Warren, 1981; Choudhury and Chang, 1981). The statistical analysis performed using the optical and reflective properties of snow formed the basis for a normalized snow index to computationally determine pixels as snow-covered. The introduction of the Normalized Difference Snow Index (NDSI) which followed the work on calculating snow spectra was based on the commonly used Normalized Difference Vegetation Index (NDVI) (Tait et al., 2001; Hall et al., 1995). These algorithms were already in place prior to the launch of NASA's Terra satellite in 1999 (Hall et al., 1995), and were updated after the launch of the second MODIS instrument aboard the Aqua satellite in 2002 (Salomonson and Appel, 2004).

Estimating snow cover through remote sensing uses the spectral reflectance of different snow types as a foundation. A series of physical experiments that measures broadband albedo of different grain sizes, impurity ratios, snow depths, and solar elevation angles provides extensive information on the factors affecting sensor perception of snow reflectance. Figure 1 shows spectral reflectance for snow types of different granularity (Wiscombe and Warren, 1981; O'Brien and Munis, 1975). Wiscombe and Warren (1981) state that the albedo of snow reaches its asymptotic limit at depths greater than just a few centimeters, as well as fresh snow usually having grain radii between 20 and 100 μm.

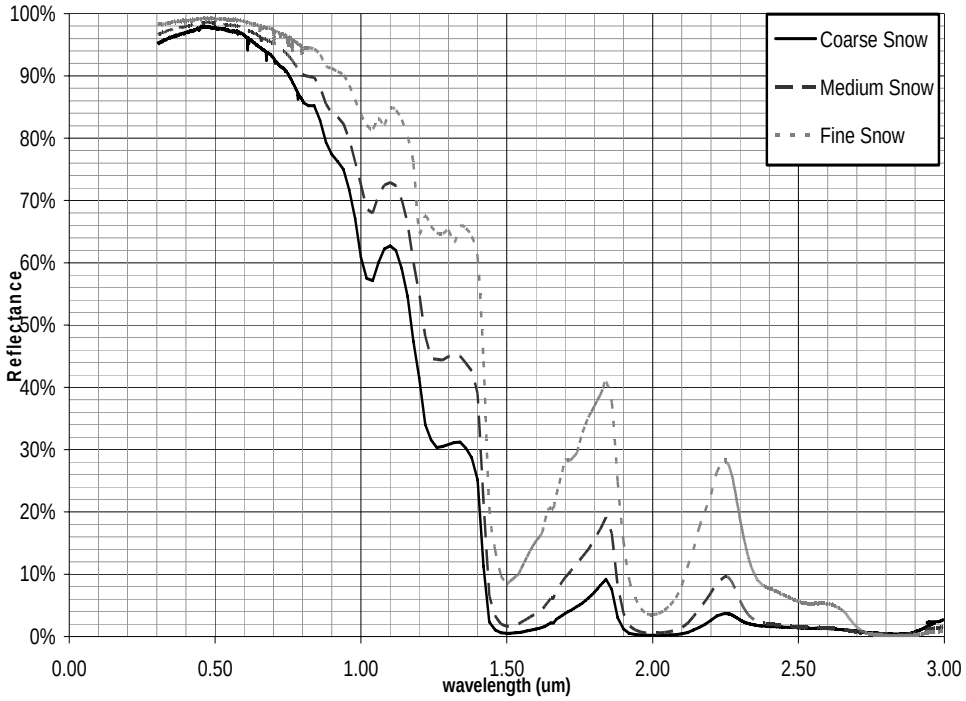

Figure 1: Reflectance Spectra for Various Snow Types. Boxes show the approximate bandwidth values for channels used in calculation of snow indices. From left to right – green (0.56 μm), red (0.66 μm), and Short-wave Infrared [SWIR] (1.65 μm). *(*adapted from Wiscombe and Warren, 1981, and O'Brien and Munis, 1975)

By creating a contrast between two bands with very different reflectance characteristics, and using standardized indices based on broadband reflective characteristics, different types of vegetation, soils, burned areas, as well as snow and ice, can be discriminated. At longer wavelengths, reflectance (ρ) measurements of snow, new and old, fine, medium and coarse, have low to extremely low albedo measurements, creating a large contrast when compared to wavelengths in the visible region. Tables 1a through 1c give the radiometric information for the MODIS and ASTER instruments, as well as the notation used throughout this paper.

Subsystem	Band Number	Spectral Range (μm)	Spatial Resolution
VNIR	A1 A2 A3N A3B	0.520 - 0.600 0.630 - 0.690 0.780 - 0.860 0.780 - 0.860	15 m
SWIR	A4 A5 A6 A7 A8 A9	1.600 - 1.700 2.145 - 2.185 2.185 - 2.225 2.235 - 2.285 2.295 - 2.365 2.360 - 2.430	30 m

Table 1a: ASTER Radiometric Properties. (USGS, 2004)

Band	Spectral Range (μm)	Spatial Resolution
M1	0.620 – 0.670	250 m
M2	0.841 – 0.876	
M3	0.459 – 0.479	500 m
M4	0.545 – 0.565	
M5	1.230 – 1.250	
M6	1.628 – 1.652	
M7	2.105 – 2.155	

Table 1b: MODIS Radiometric Properties. (NASA GSFC, 2007)

Abbreviation	Approximate Wavelengths	MODIS (M) Channel	ASTER (A) Channel
Green	0.520 - 0.605 μm	M4	A1
Red	0.630 - 0.690 μm	M1	A2
SWIR (Short-Wave Infrared)	1.550 - 1.750 μm	M6	A4

Table 1c: Reference tables for shorthand notation used throughout this document.

NDSI is defined as: (Hall et al., 1995, 1998)

$$NDSI_{MODIS} = (\rho_{M4} - \rho_{M6}) / (\rho_{M4} + \rho_{M6}) \quad (1)$$

$$NDSI_{ASTER} = (\rho_{A1} - \rho_{A4}) / (\rho_{A1} + \rho_{A4}) \quad (2)$$

where M and A refer to the specific instrument (MODIS or ASTER), and the numbers 1, 4, and 6 refer to the respective band number used to generate values for each index. More recently, a slight variation on the original NDSI has come into practice. Employing the same principles, the Normalized Difference Snow/Ice Index (NDSII), sometimes referred to as $NDSI_{red}$ versus $NDSI_{green}$, has been used for the same type of snow analysis (Xiao et al., 2004). For MODIS data, the index would use bands 1 and 6 as shown in equation 3. Similar results would be expected from the corresponding bands of ASTER data.

$$NDSII_{MODIS} = (\rho_{M1} - \rho_{M6}) / (\rho_{M1} + \rho_{M6}) \quad (3)$$

$$NDSII_{ASTER} = (\rho_{A2} - \rho_{A4}) / (\rho_{A2} + \rho_{A4}) \quad (4)$$

When comparing the data available for download from each of these instruments, MODIS is by far the easiest to use for computational purposes. MODIS data is available at multiple levels of processing and free to any individual with access to the public internet database. Multiple levels of remote sensing products are available for the ASTER instrument; however, with a reduced database size, most high-level products (e.g. vegetative indices, calibrated reflectance) must be purchased on a per scene basis.

AREA OF INTEREST

The five scenes analyzed were acquired over the Great Lakes region in the central United States (Figure 2). Table 4 gives temporal and geographical information on the five scenes used for the complete research, using the ASTER data as a basis.

***Figure 2**:* Map of Great Lakes Region of the United States, showing the locations of the five scenes analyzed. Scenes lettered in chronological order starting with Scene A in upstate New York (February 16, 2004) and ending with Scene E in central Illinois (December 2, 2005). Information for each of these scenes can be found in Table 2. (Hulka, 2007)

This area is often used for snow-cover analysis and weather forecasting because it has a significant effect on the region's weather, especially with regard to lake-effect snow. This, coupled with varied topographical features including mountain ranges, make this region a unique area to study winter precipitation as well as its distribution and impact on the hydrologic cycle.

Scene	Year	Month	Day	Time (UTC) (hms)	Bands (RGB)
A	2004	2	16	16 03 22	A2, A1, A4
B	2005	1	27	16 39 04	A2, A1, A4
C	2005	1	27	16 39 30	A2, A1, A4
D	2005	3	21	16 57 30	A2, A1, A4
E	2005	12	2	16 58 12	A2, A1, A4

Scene	Upper Left Coordinate	Lower Right Coordinate
A	(+43.303, -75.435)	(+42.873, -74.848)
B	(+43.305, -84.611)	(+42.873, -84.022)
C	(+41.681, -85.050)	(+41.297, -84.576)
D	(+44.605, -90.647)	(+44.173, -90.045)
E	(+40.569, -89.486)	(+40.137, -88.921)

Table 2: Geographical, spectral and temporal information for the five analyzed scenes. Locations of these scenes are indicated in Figure 2.

GUIDING EQUATIONS

Data from the ASTER granules is stored initially as Digital Numbers (DN) and requires a rather simple conversion to produce a value of radiance ($\mathbf{L}_\lambda$), shown in Equation 5.

$$L_\lambda = gain * (DN - 1) \qquad (5)$$

where DN values range from 1 to 255. The metadata attached to the Hierarchical Data File (HDF) includes information on which gain settings to use for each band. For each scene, the metadata indicates using the high gain settings for the visible bands, and the normal gain settings for all others. In contrast, the MOD02 datasets (Calibrated Radiance and Reflectance) available through the NASA Goddard Space Flight Center website already have the conversions done, as well as a cloud-mask correction applied to the distributed dataset. The user is required to do these same conversions manually with ASTER data and co-reference the scenes in order to perform an accurate analysis.

Once radiance has been calculated, constants are input in order to convert this value to reflectance ($\rho_\mathbf{p}$).

$$\rho_p = \frac{\pi * L_\lambda * d^2}{ESUN_\lambda * \cos\theta_s} \qquad (6)$$

where ***d*** is the Earth-Sun distance in astronomical units. This value is nearly a constant (1) throughout the year, yet has a small but quantifiable effect on the resulting reflectance. $\boldsymbol{ESUN}_\lambda$ refers to the mean top-of-atmosphere solar irradiance values. Reference values of both are available in standard reference tables (NASA GSFC/Landsat 7, 2006). The angle θ_s is the solar zenith angle.

Each co-referenced ASTER-MODIS scene comparison was completed in a similar manner. Since the comparison for this study involved co-referenced ASTER and MODIS scenes using the original MODIS data at 500-m and the ASTER data aggregated to the equivalent resolution, ASTER granules were re-sampled to 25-meter resolution, and an aggregate set was created at resolutions of 50-m, 100-m and 250-m, and 500-m MODIS 'equivalent' datasets. Figure 3 outlines the procedures followed in this analysis. File types are listed, but different software packages can be used for a similar replication of this analysis for the same datasets or different ones.

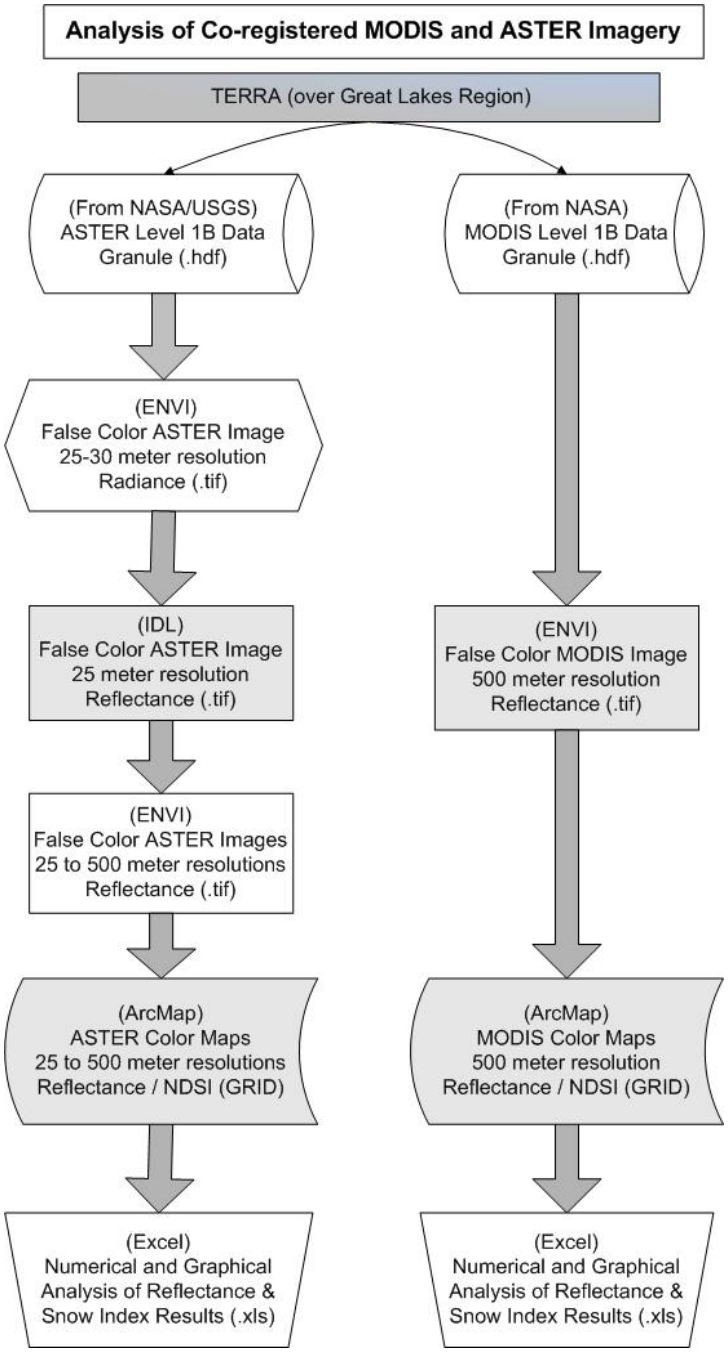

Figure 3: Chart of principles, procedures and data used in comparing co-referenced MODIS and ASTER scenes for snow-cover analysis. File types are noted in parentheses, but various software packages can carry out these basic computations and statistical analyses. (Hulka, 2007)

RESULTS AND DISCUSSION

Figures 4a, 4b, and 4c show the reflectance versus digital number (DN) comparing the normal and high gain settings for each of the three ASTER bands used. Figures 5a, 5b, and 5c show the difference for a real dataset (Scene B) between the gain settings listed for use in the ASTER metadata file and the user-adjusted gain settings, as well as the original 500-m MODIS data.

Datasets listed as using corrected or adjusted gain settings used a floor of 0.01% and a ceiling of 100.0% as limits. The number of negative pixels replaced with minimum (0.01%) values and excessive (>100%) values replaced with 100.0% totaled fewer than 100 (at 500-m resolution) for each of the five images, or less than 0.01% of the total.

Table 3a lists the high and normal gain settings for ASTER bands A1, A2, and A4. The shaded boxes indicate the settings listed in the attached metadata file for each scene. Table 3b shows the exact gain values used for each band of the five scenes analyzed. For all scenes, simply using the normal gain for the red band (A2) instead of the high gain produces physically representative reflectance values for snow, as most pixels have reflectance values above 80%, with the largest 5% cluster being the 95th percentile – a typical snow signature. Prior to this adjustment, most reflectance values are between 45% and 50% with a maximum just above 50%.

Band	High	Normal
A1	0.676	1.688
A2	0.708	1.415
A4	0.1087	0.2174

Table 3a: Gain settings for ASTER channels used in this analysis. Shaded boxes indicate gain values listed for use in each metadata file. (Tsuchida et al., 2004)

	A	B	C	D	E
Green (A1)	1.688	1.688	1.801	1.818	1.688
Red (A2)	1.415	1.415	1.415	1.415	1.415
SWIR (A4)	0.0967	0.0757	0.0392	0.1181	0.0725

Table 3b: Actual gain settings for ASTER channels used in analysis for each scene. SWIR (Channel A4) gain values were adjusted to properly represent reflectance values for snow.

Using the green (A2) band produced similar results. Uncorrected reflectance values peaked around 40%. For two of the scenes, using the normal gain setting worked adequately for matching the snow signature. The other three scenes (C through E) required further adjustment for snow spectra, data predominantly indicating a 90% or greater reflectance for most of the pixels in the image.

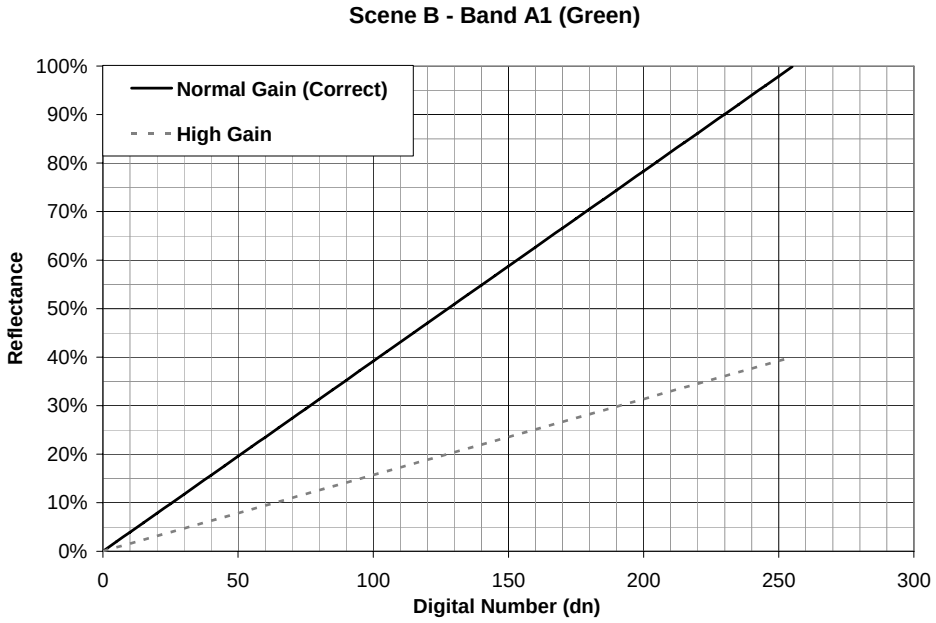

Figure 4a: Comparison of the expected green reflectance as a function of possible digital number counts for Scene B. Using the high gain value of 0.676, a maximum DN count will only result in a reflectance of no higher than 40%. The corrected line uses the normal gain value of 1.688 and produced a more accurate range of resulting reflectance.

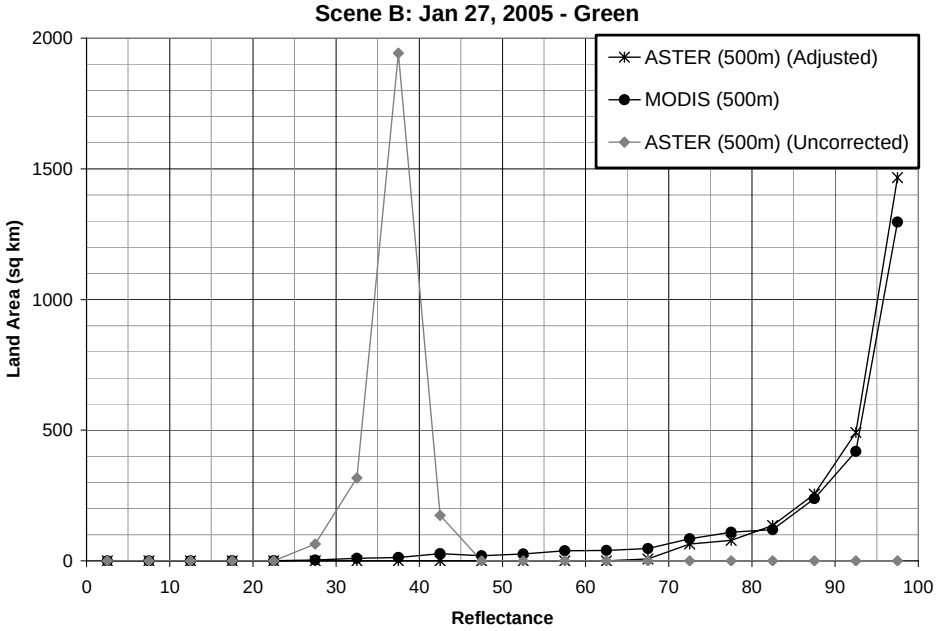

***Figure 5a**:* Green reflectance for ASTER-aggregated and MODIS data at 500-meter resolution, grouped into 5% clusters. The uncorrected line uses the listed high gain of 0.676 for this channel. The adjusted line uses the normal gain value of 1.688, as listed in Table 3b.

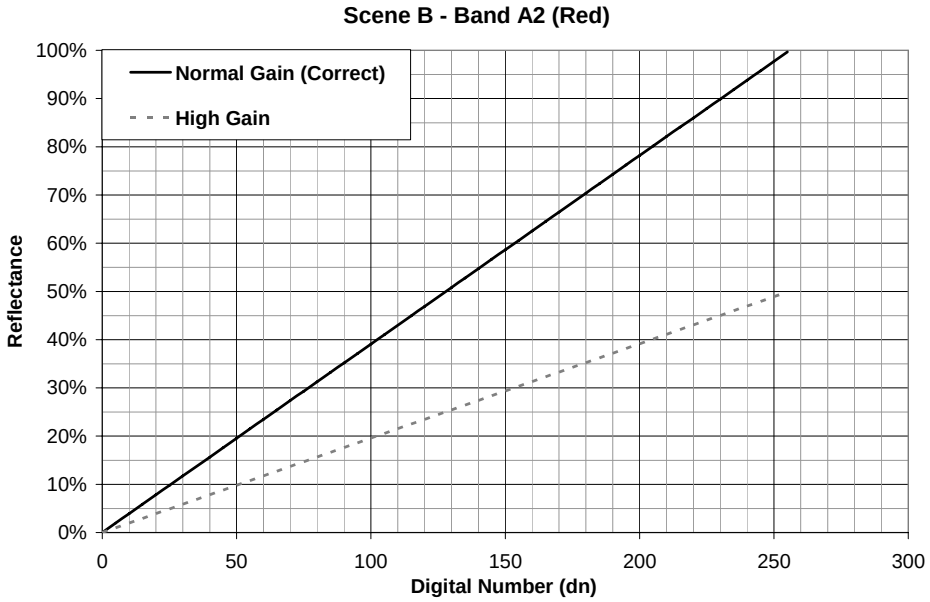

Figure 4b: Comparison of the expected red reflectance as a function of possible digital number counts for Scene B. Using the high gain value of 0.708, a maximum DN count will only result in a reflectance of no higher than 50%. The corrected line uses the normal gain value of 1.415 and produced a more accurate range of resulting reflectance.

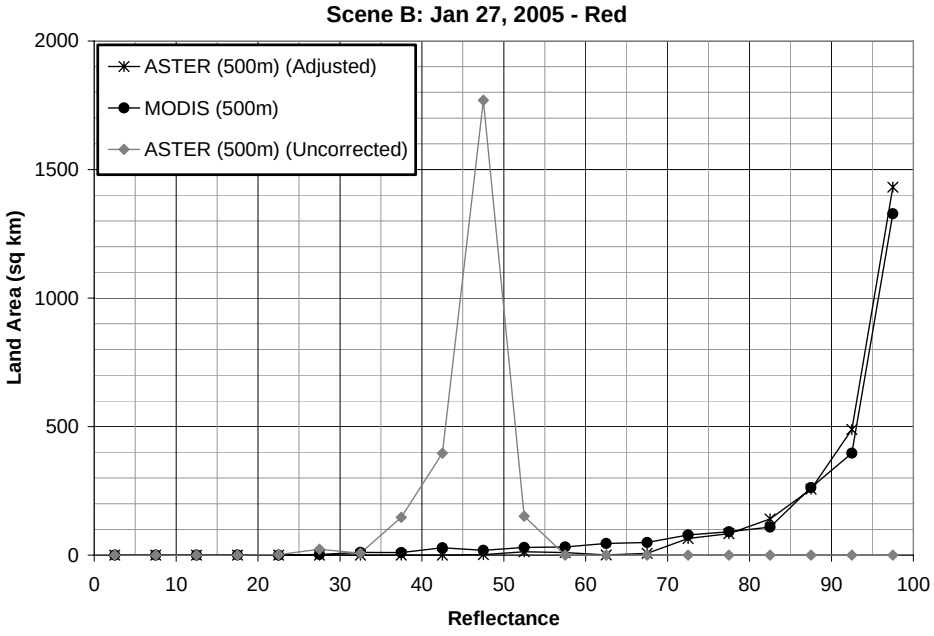

Figure 5b: Red reflectance for ASTER-aggregated and MODIS data at 500-meter resolution, grouped into 5% clusters. The uncorrected line uses the listed high gain of 0.708 for this channel. The adjusted line uses the normal gain value of 1.415, as listed in Table 3b.

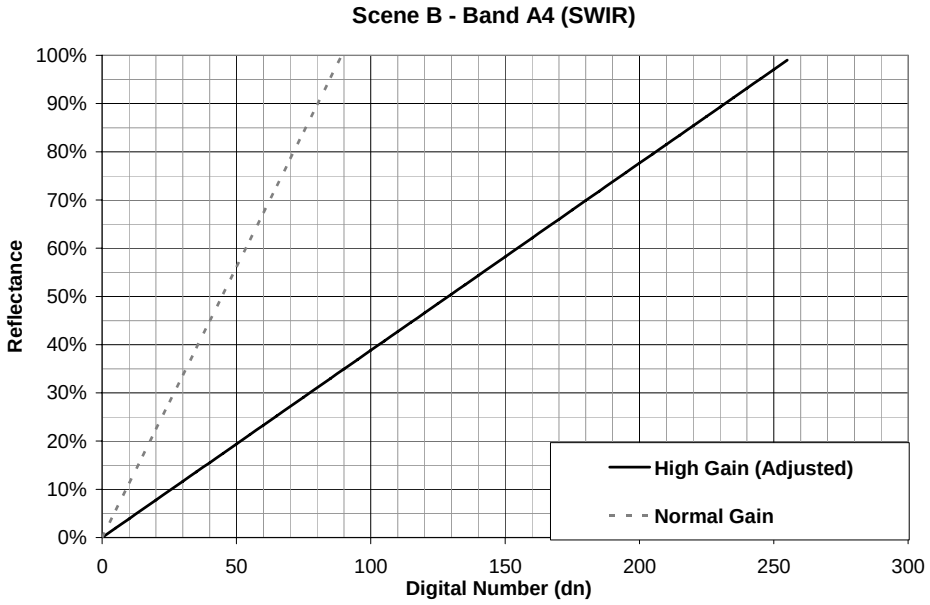

Figure 4c: Comparison of the expected SWIR reflectance as a function of possible digital number counts for Scene B. Using the normal gain value of 0.2174, a maximum DN count will only result in a reflectance of much greater than 100%. The corrected line uses the gain value of 0.0757 and produces a more accurate range of resulting reflectance.

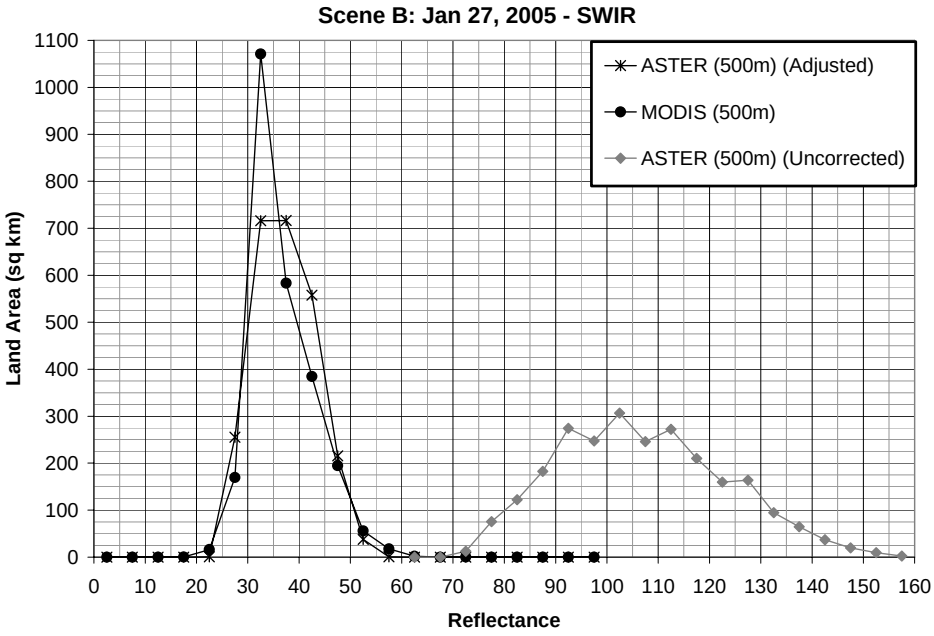

Figure 5c: SWIR Reflectance for ASTER-aggregated and MODIS data at 500-meter resolution, grouped into 5% clusters. The uncorrected line uses the listed normal gain of 0.2174 for this channel. The adjusted line uses a gain value of 0.0757, as listed in Table 3b.

The opposite was found for the Short-Wave Infrared (SWIR) band. The gain settings listed in the metadata consistently produced physically impossible reflectance values of greater than 100% for almost the entire image. Figure 5c shows the comparison between the corrected and uncorrected reflectance distributions in addition to the distribution for the MODIS scene. In general, the reflectance distribution graphs matched up much better between ASTER and MODIS for the visible bands as compared to the infrared band. Also noticeable is that each scene required secondary adjustments to the gain settings in order to produce results typical of snow in the infrared range.

It is impractical to use ground truth verification for snow reflectance from remote sensors. Corrections can be applied for attenuation of the reflected signal between the ground and the satellite, but factoring in the mixing of other background albedos in a 500-meter-square pixel alters the reflectance at the sensor. The temporal simultaneity of ASTER and MODIS is an advantage that is extremely useful for snow cover analysis as well as monitoring other land surface processes. NDSI is a useful tool because it is a scale-independent algorithm. Using a universally accepted process on multiple simultaneous datasets at different scales can only help improve accuracy when results are compared and contrasted.

CONCLUSIONS

Analyzing snow cover is a complex process involving precision issues with regard to measurement. While ground reporting of snowfall is still a common and effective practice, these are point measurements, often interpolated to create snow cover maps. The NWS Cooperative Observer (CO-OP) network consists of a series of over ten thousand voluntary reporting stations throughout the continental United States, although snow depth is not calculated at every site (Maurer et al., 2003). The US Natural Resources Conservation Service SNOpack TELemetry (SNOTEL) is focused more on the western United States in mountain ranges and major river basins.

Cold weather fronts that bring precipitation in the form of snow can cover significant geographic regions in the span of a few hours to a few days. However, the depth, granularity, and water content of a snow pack can vary greatly over much shorter distances. MODIS is an effective tool because the 500-m resolution of the sensor can cover large areas of continents at one time. The data is readily available with atmospheric corrections and pre-processing into a usable quantity (radiance or reflectance) is already done prior to distribution to end users.

ASTER, and previously LANDSAT, has provided users more interested in local snowfall analysis better resolution to analyze changes in the hydrologic cycle. Being able to determine the edge of a melting snow pack on the side of a mountain in early spring would more easily be determined using a 30-m ASTER or LANDSAT image in comparison to a 500-m MODIS image.

The advantage of using ASTER instead of LANDSAT is that the user can compare the scene to one from MODIS-Terra, because the instruments capture images from the same area at the same time. The same analysis can be done for LANDSAT, but finding a co-referenced scene at the same exact time would be nearly impossible – so there is no real means for verification of the results.

The calibration of the data into a useful format for calculating snow cover using NDSI or NDSII requires scene-specific adjustments to the data to make it as useful as MODIS data would be immediately after user-acquisition. In addition, this method requires another method of verifying that the user-changes to the calibration parameters for each scene are verifiable. The method of co-referencing high-resolution ASTER data with a MODIS scene and aggregating the high-resolution data to an equivalent 500-m resolution was effective in providing verification that reflectance values are physically representative of snow. This enables scientists to use NDSI for high resolution ASTER scenes and ensure that the index values are accurate.

Acknowledgements

This research was made possible directly and indirectly through funding from the South Dakota Space Grant courtesy of Tom Durkin under NASA Training Grant NNG05GJ98H, and from Richard Farley under NOAA Health Grant WRAF-060-4. Others who contributed during the research and writing process at the Institute of Atmospheric Sciences at the South Dakota School of Mines and Technology were Matthew Beals, William Capehart, Pam Cox, Connie Crandall, Edward Duke, Donna Kliche, Patrick Kozak, and Patrick Zimmerman. Additional thanks for continued writing and editing support to Louis Scuderi at the Department of Earth and Planetary Sciences at the University of New Mexico under NASA Grant NNS04AB25G.

BIBLIOGRAPHY

CHOUDHURY, B.J., and CHANG, A.T.C., 1981, The albedo of snow for partially cloudy skies. *Boundary Layer Meteorology,* **20**; 371-389.

HALL, D.K. and MARTINEC, J., 1985. *Remote Sensing of Ice and Snow*. Chapman and Hall Ltd, New York, 189.

HALL, D.K., FOSTER, J.L., VERBYLA, D.L., KLEIN, A.G., and BENSON, C.S., 1998, Assessment of Snow-Cover Mapping Accuracy in a Variety of Vegetation-Cover Densities in Central Alaska. *Remote Sensing of Environment,* **66**; 129-137.

HALL, D.K., RIGGS, G.A., and SALOMONSON, V.V., 1995, Development of Methods for Mapping Global Snow Cover Using Moderate Resolution Imaging Spectroradiometer Data. *Remote Sensing of Environment,* **54**; 127-140.

HULKA, J. R., 2007. *A Multi-Scale Remote Sensing Analysis of Great Lakes Snowfall.* Master's Thesis, South Dakota School of Mines and Technology, Rapid City, South Dakota, 123 p.

MAURER, E. P., RHOADS, J. D., DUBAYAH, R. O., and LETTENMAIER, D. P., 2003, Evaluation of the snow-covered area data product from MODIS. *Hydrological Processes,* **17***,* 59-71

NASA Goddard Space Flight Center (GSFC), 2006. *Landsat 7 Science Data Users Handbook. Chapter 11 – Data Products.*. Retrieved September 29, 2007, from

http://landsathandbook.gsfc.nasa.gov/handbook/handbook_htmls/chapter11/chapter11.html

NASA Goddard Space Flight Center (GSFC), 2007. *Components of MODIS.* Retrieved September 29, 2007, from *http://modis.gsfc.nasa.gov/about/specifications.php*

O'BRIEN, H. W. and MUNIS, R. H., 1975, Red and near-infrared spectral reflectance of snow. In *Operational Applications of Satellite Snowcover Observations (ed. A. Rango),* Proceedings of a workshop held in South Lake Tahoe, CA, 18-20 August 1975, NASA, Washington, DC, NASA SP-391*,* pp. 345-360.

ROBINSON, D.A., DEWEY, K.F., and HEIM, Jr, R.R., 1993, Global Snow Cover Monitoring: An Update. *Bulletin of the American Meteorological Society,* **74**; 1689-1696.

SALOMONSON, V.V., and APPEL, I., 2004, Estimating fractional snow cover from MODIS using the normalized difference snow index. *Remote Sensing of Environment,* **89**; 351-360.

TAIT, A. B., BARTON, J. S., and HALL, D.K., 2001, A prototype MODIS-SSM/I snow-mapping algorithm. *International Journal of Remote Sensing,* **22**; 3275-3284.

TSUCHIDA, S., SAKUMA, H., and IWASAKI, A., 2004, *Equations for ASTER radiometric calibration ver.0.20*. National Institute of Advanced Industrial Science and Technology (Japan).

US GEOLOGICAL SURVEY. Land Processes Distributed Active Archive Center (LP DAAC), 2004. *An Overview of ASTER.* Retrieved September 29, 2007, from

http://edcdaac.usgs.gov/aster/asteroverview.asp#baseline

WISCOMBE, W. J., and WARREN, S. G., 1981, A Model for the Spectral Albedo of Snow. I: Pure Snow. *Journal of Atmospheric Sciences,* **37**; 2712-2733.

XIAO, X., ZHANG, Q., BOLES, S., RAWLINS, M., and MOORE III, B., 2004, Mapping snow cover in the pan-Arctic zone, using multi-year (1998-2001) images from optical VEGETATION sensor. *International Journal of Remote Sensing,* **22**; 5732-5744.